Phys. Lett. B 865 (2025) 139451

Contents lists available at ScienceDirect

Physics Letters B

journal homepage: www.elsevier.com/locate/physletb

Letter

Kaon distribution functions from empirical information

Zhen-Ni Xu (徐珍妮) [a], Daniele Binosi [b], Chen Chen (陈晨) [c,d], Khépani Raya [a], Craig D. Roberts [e,f,*], José Rodríguez-Quintero [a,g]

[a] Department of Integrated Sciences and Center for Advanced Studies in Physics, Mathematics and Computation, University of Huelva, E-21071 Huelva, Spain
[b] European Centre for Theoretical Studies in Nuclear Physics and Related Areas (ECT*), Villa Tambosi, Strada delle Tabarelle 286, I-38123 Villazzano (TN), Italy
[c] Interdisciplinary Center for Theoretical Study, University of Science and Technology of China (USTC), Hefei, Anhui 230026, China
[d] Peng Huanwu Center for Fundamental Theory (PCFT), Hefei, Anhui 230026, China
[e] School of Physics, Nanjing University, Nanjing, Jiangsu 210093, China
[f] Institute for Nonperturbative Physics, Nanjing University, Nanjing, Jiangsu 210093, China
[g] Irfu, CEA, Université de Paris-Saclay, 91191, Gif-sur-Yvette, France

ARTICLE INFO

Editor: A. Ringwald

Keywords:
Continuum Schwinger function methods
Drell-Yan reactions
Emergence of mass
Meson structure functions
Nambu-Goldstone bosons
Parton distribution functions

ABSTRACT

Using available information from Drell-Yan data on pion and kaon structure functions, an approach is described which enables the development of pointwise profiles for all pion and kaon parton distribution functions (DFs) without reference to theories of hadron structure. The key steps are construction of structure-function-constrained probability-weighted ensembles of valence DF replicas and use of an evolution scheme for parton DFs that is all-orders exact. The DFs obtained express qualitatively sound features of light-meson structure, *e.g.*, the effects of Higgs boson couplings into QCD and the size of heavy-quark momentum fractions in light hadrons. In order to improve the results, additional and more precise data on the u-quark-in-kaon, u^K, to u-quark-in-pion, u^π, DF ratio would be necessary. Of greater value would be extraction of u^K alone, thereby avoiding inference from the ratio: currently, the data-based form of u^K is materially influenced by results for u^π.

1. Introduction

The kaon was identified via a series of observations that began more than seventy years ago [1–4]. Today, it is known to be a dichotomous system, *viz*. both a bound state seeded by a light quark/antiquark and a strange antiquark/quark and, like the pion, first seen around the same time [5], a Nambu-Goldstone boson. For instance, the valence content of the K^+ is $u\bar{s}$. Moreover, the fascinating dichotomy can be resolved by exploiting the impact of interference between Nature's two known sources of mass generation; namely, Higgs boson couplings into QCD and emergent hadron mass (EHM) [6–11]: pions and kaons are keys in the effort to elucidate EHM phenomena.

Data relating to pion structure are limited [12], but the kaon case is dire; so, validating any picture of the kaon is especially difficult. In fact, even after seventy years, practically nothing is known about kaon structure, *e.g.*, the precision of charged kaon elastic electromagnetic form factor, F_K, measurements is such that no objective result for the kaon charge radius is available [13], the evolution of F_K with squared momentum-transfer, Q^2, is uncertain [14], and only eight points relating to in-kaon parton distribution functions (DFs) are available [15]. These difficulties stem from the short lifetime of the kaon and its relatively low production rate. The situation is expected to be improved in the coming decades by exploiting the capacity of high-luminosity, high-energy accelerators [6,16–20]. In the interim, it is worth determining what can be inferred from existing kaon data and thereby highlight some of the insights that new data should bring. Such information should also provide useful benchmarks for contemporary phenomenology and theory of Nambu-Goldstone boson structure, which, following recognition of its role as a clear window onto EHM, is receiving much attention – see, *e.g.*, Refs. [21–32].

2. DF evolution and the hadron scale

To be concrete, we will speak of the K^+. Apart from changing $u \to \bar{u}$, $\bar{s} \to s$, all remarks pertain equally to K^-. So, denote the valence DFs of the K^+ by $q^K(x;\zeta)$, where $q = u, \bar{s}$, x is the light-front fraction of the kaon's four-momentum carried by the indicated valence species, and ζ is the scale at which this fraction is resolved. Any such DF is fully characterised by its Mellin moments ($m \in \mathbb{Z}^>$):

* Corresponding author.
E-mail addresses: chenchen1031@ustc.edu.cn (C. Chen), cdroberts@nju.edu.cn (C.D. Roberts), jose.rodriguez@dfaie.uhu.es (J. Rodríguez-Quintero).

https://doi.org/10.1016/j.physletb.2025.139451
Received 3 December 2024; Received in revised form 6 March 2025; Accepted 3 April 2025
Available online 4 April 2025

$$\langle x^m\rangle^{\zeta}_{q^K} = \int_0^1 dx\, x^m q^K(x;\zeta)\,, \tag{1}$$

with $\langle x^0\rangle^{\zeta}_{q^K} = 1$ owing to baryon number conservation.

The relation between DFs at different resolving scales is given by the DGLAP equations [33–36]. Herein, we exploit the all-orders (AO) scheme detailed in Ref. [37], which is built upon the following two propositions. (*I*) There is an effective charge, $\alpha_{1\ell}(k^2)$, of the type explained in Refs. [38,39] and reviewed in Ref. [40], that, when used to integrate the leading-order perturbative DGLAP equations, defines an evolution scheme for *every* parton DF that is all-orders exact. The pointwise form of $\alpha_{1\ell}(k^2)$ is largely immaterial. Nonetheless, the process-independent QCD running coupling calculated in Refs. [41] has all required properties. (*II*) There is a scale, $\zeta_{\mathcal{H}}$, whereat all properties of a given hadron are carried by its valence degrees-of-freedom. At $\zeta_{\mathcal{H}}$, DFs associated with glue and sea quarks are zero. Working with the charge discussed in Refs. [40–42], the value of the hadron scale is a prediction [43]: $\zeta_{\mathcal{H}} = 0.331(2)\,\text{GeV}$. A consistent value, $\zeta_{\mathcal{H}} = 0.350(44)\,\text{GeV}$, is obtained from an analysis of lattice-QCD (lQCD) results relating to the pion valence quark DF [44].

The AO approach defines a nonperturbative extension of DGLAP evolution. It has successfully been used in many applications, *e.g.*, delivering unified predictions for pion fragmentation functions [45] and all pion, kaon, and proton DFs [22,46–49], a viable species separation of nucleon gravitational form factors [50], and insights into quark and gluon angular momentum contributions to the proton spin [51].

Within the AO scheme,

$$\langle x\rangle^{\zeta_{\mathcal{H}}}_{u^K} + \langle x\rangle^{\zeta_{\mathcal{H}}}_{\bar{s}^K} = 1\,; \tag{2}$$

hence $\bar{s}^K(x;\zeta_{\mathcal{H}}) = u^K(1-x;\zeta_{\mathcal{H}})$ and

$$\mathcal{K}(x;\zeta_{\mathcal{H}}) = \tfrac{1}{2}[u^K(x;\zeta_{\mathcal{H}}) + \bar{s}^K(x;\zeta_{\mathcal{H}})] = \mathcal{K}(1-x;\zeta_{\mathcal{H}})\,. \tag{3}$$

Working with this symmetric DF, one may capitalise on both the Mellin moment physical bounds and recursion relation presented in Ref. [52].

Predictions for hadron scale valence DFs in the pion and kaon are available [22]. For practical purposes, they can be interpolated using the following function:

$$q^M(x;\zeta_{\mathcal{H}}) = n_0 \ln\left[1 + x^2(1-x)^2/\rho_M^2\right][1 \pm \gamma_M(1-2x)]\,, \tag{4}$$

$M = \pi, K$, where $n_0 = n_0(\rho_M)$ ensures $\langle x^0\rangle^{\zeta}_{q^M} = 1$, $\gamma_\pi = 0$, and, in the kaon, one has "$+\gamma_K$" for the u quark and "$-\gamma_K$" for the $\bar{s}$. Equally good interpolations are obtained using

$$u^M(x;\zeta_{\mathcal{H}}) = \tilde{n}_0 \ln\left[1 + x^2(1-x)^2(1+\tilde{\gamma}_M^2 x^2(1-x)^4)/\tilde{\rho}_M^2\right]\,, \tag{5}$$

with $\tilde{n}_0 = n_0(\tilde{\rho}_M, \tilde{\gamma}_M)$, $\tilde{\gamma}_\pi = 0$, $\bar{s}^K(x;\zeta_{\mathcal{H}}) = u^K(1-x;\zeta_{\mathcal{H}})$. Both forms respect the $x \simeq 0, 1$ endpoint behaviour predicted by continuum analyses of the meson bound state problem that preserve an identifiable connection with a gluon exchange interaction between valence degrees of freedom [6, Sec. 5.A]. Moreover, for any $\rho_M > 0$, they express the EHM-induced dilation that is a characteristic feature of π, K DFs [6,8,32]; and with $\gamma_K \neq 0$ (equivalently, $\tilde{\gamma}_K \neq 0$), the skewing introduced by Higgs boson couplings into QCD is preserved [23]. For our purposes, Eq. (4) is easier to work with, but it is better to use Eq. (5) when considering fragmentation functions [45]. This is not an issue because one may readily map $(\rho_M, \gamma_M) \to (\tilde{\rho}_M, \tilde{\gamma}_M)$; so, pass between the two forms without information loss.

Using Eq. (4), one has

$$\langle x^m\rangle^{\zeta_{\mathcal{H}}}_{q^K}(\rho_K, \gamma_K) = \langle x^m\rangle^{\zeta_{\mathcal{H}}}_{\mathcal{K}} \pm \gamma_K(\langle x^m\rangle^{\zeta_{\mathcal{H}}}_{\mathcal{K}} - 2\langle x^{m+1}\rangle^{\zeta_{\mathcal{H}}}_{\mathcal{K}})\,, \tag{6}$$

where the subscript $\mathcal{K}$ indicates a moment of the symmetrised DF in Eq. (3). For $m = 1$, with kaon DF skewing measured via $\delta_K = 1/2 - \langle x\rangle^{\zeta_{\mathcal{H}}}_{u_K} = \langle x\rangle^{\zeta_{\mathcal{H}}}_{\bar{s}_K} - 1/2$,

$$\gamma_K = 2\delta_K/[4\langle x^2\rangle^{\zeta_{\mathcal{H}}}_{\mathcal{K}} - 1]\,. \tag{7}$$

3. DFs at empirical scales

An interpretation of experimental data in terms of parton DFs is only possible at resolving scales $\zeta \gg \zeta_{\mathcal{H}}$. In this connection, the strength of the AO scheme becomes manifest because one finds [37, Eq. (9)]:

$$\langle x^m\rangle^{\zeta}_{\mathcal{K}}/\langle x^m\rangle^{\zeta_{\mathcal{H}}}_{\mathcal{K}} = [\langle 2x\rangle^{\zeta}_{\mathcal{K}}]^{\gamma_0^m/\gamma_0^1}\,, \tag{8}$$

where

$$\gamma_0^n = -\frac{4}{3}\left[3 + \frac{2}{(n+1)(n+2)} - 4\sum_{k=1}^{n+1}\frac{1}{k}\right]\,, \tag{9}$$

so $\gamma_0^0 = 0$, and all other anomalous dimensions may be found in Ref. [37, Eq. (6)]. Equation (8) is the statement that given the symmetrised valence quark DF in Eq. (3), then its pointwise form at any $\zeta > \zeta_{\mathcal{H}}$ is completely determined by its $m = 1$ moment at that scale. It is further worth recording that, ignoring quark current-mass dependence in the splitting kernels, which is a good approximation for π and K mesons [22]:

$$\forall \zeta > \zeta_{\rm H} \,|\, \langle 2x\rangle^{\zeta}_{\mathcal{K}} = \langle 2x\rangle^{\zeta}_{u_\pi} = \langle x\rangle^{\zeta}_{q_K}/\langle x\rangle^{\zeta_{\mathcal{H}}}_{q_K} < 1 \tag{10}$$

and

$$\langle x^m\rangle^{\zeta}_{q^M}/\langle x^m\rangle^{\zeta_{\mathcal{H}}}_{q^M} = [\langle 2x\rangle^{\zeta}_{u^\pi}]^{\gamma_0^m/\gamma_0^1}\,. \tag{11}$$

The following function is a commonly used parametrisation of valence DFs at $\zeta > m_p$, where m_p is the proton mass:

$$q^M(x;\zeta) = N_0(\alpha, \beta, c_q^M)\, x^{\alpha-1}(1-x)^\beta\left(1 + c_q^M\, x^2\right)\,. \tag{12}$$

Here, N_0 ensures unit normalisation for the $m = 0$ DF moment and the parameters (α, β, c_q^M) depend on ζ. It is straightforward to establish that

$$c_{q,\zeta}^M = -\frac{(2+\alpha+\beta)(3+\alpha+\beta)(\alpha - (1+\alpha+\beta)\langle x\rangle^{\zeta}_{q^M})}{\alpha(1+\alpha)(2+\alpha-(3+\alpha+\beta)\langle x\rangle^{\zeta}_{q^M})}\,. \tag{13}$$

Under flavour-independent nonsinglet AO evolution, α and β evolve separately, but in the same way for all mesons and from the same starting point, *i.e.*, the values $\alpha(\zeta)$, $\beta(\zeta)$ are each generated from hadron scale DFs with $\alpha(\zeta_{\mathcal{H}}) = 3$, $\beta(\zeta_{\mathcal{H}}) = 2$ – see Eq. (4). Hence, u^K/u^π is a nonzero finite number at $x = 0, 1$:

$$u^K/u^\pi\big|^{\zeta}_{x=0} = \frac{2+\alpha-(3+\alpha+\beta)\langle x\rangle^{\zeta}_{u^K}}{2+\alpha-(3+\alpha+\beta)\langle x\rangle^{\zeta}_{u^\pi}}\,, \tag{14a}$$

$$u^K/u^\pi\big|^{\zeta}_{x=1} = \frac{\alpha(4+2\alpha+\beta)-(3+\alpha+\beta)(2+2\alpha+\beta)\langle x\rangle^{\zeta}_{u^K}}{\alpha(4+2\alpha+\beta)-(3+\alpha+\beta)(2+2\alpha+\beta)\langle x\rangle^{\zeta}_{u^\pi}}\,. \tag{14b}$$

It should be stressed that Eqs. (14) are only applicable on some domain $\zeta > m_p$; namely, when Eq. (12) provides a good representation of the pointwise form of the valence quark DFs.

Given that the light-front momentum fraction carried by valence quarks vanishes as $m_p/\zeta \to 0$, then $u_K/u_\pi\big|_{x=0} \to 1$ on this scale domain: singlet DFs become dominant on $x \simeq 0$. Furthermore, $u^K/u^\pi\big|_{x=1} < 1$ for $\langle x\rangle^{\zeta}_{u^K} < \langle x\rangle^{\zeta}_{u^\pi}$, which is predicted by all studies with a sound implementation of Higgs boson couplings into QCD [23]. Both these predictions are compatible with the (sparse) available data [15]. An illustration is readily extracted from the DFs calculated in Ref. [22], the $\zeta = \zeta_5 = 5.2\,\text{GeV}$ results for which may be expressed using Eq. (12) with $\alpha = 0.88$, $\beta = 2.52$ and $\langle x\rangle^{\zeta_{\mathcal{H}}}_{u^K} = 0.47$, $\langle 2x\rangle^{\zeta_5}_{u^\pi} = 0.44$, to find

$$u^K/u^\pi\big|^{\zeta_5}_{x=0} = 1.06\,, \quad u^K/u^\pi\big|^{\zeta_5}_{x=1} = 0.66\,. \tag{15}$$

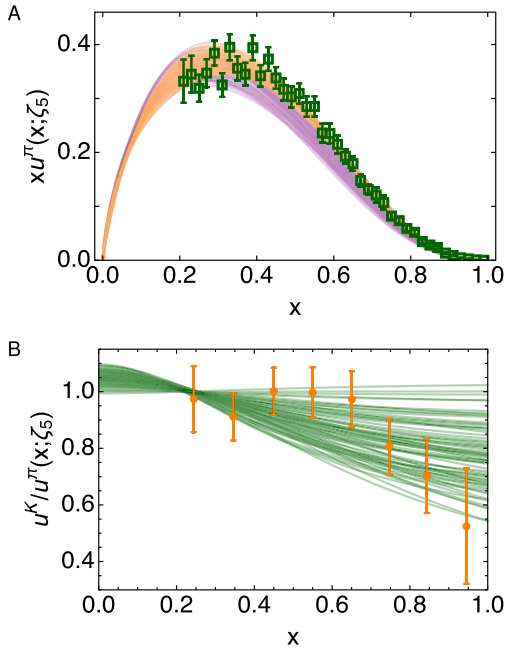

Fig. 1. Pion and kaon structure functions. Panel A. Pion (purple) and kaon (orange) ensembles of valence u quark DF replicas. Points (green): analysis of Ref. [53, E615] Drell-Yan data discussed in Refs. [43,54,55]. Panel B. Replicas for K^-/π^- u quark DF ratio (green curves). Points (orange): analysis of Drell-Yan data in Ref. [15].

4. Exploiting available data

So far as pion and kaon DFs are concerned, two practicable data sets are available, *viz.* π-induced Drell-Yan reaction cross-sections that may be understood with regard to $u^\pi(x;\zeta_5)$ [53, E615] and Drell-Yan measurements that can be interpreted in terms of the K^-/π^- structure function ratio at this same scale [15], *i.e.*, $u^K(x;\zeta_5)/u^\pi(x;\zeta_5)$. The analysis of E615 data discussed in Refs. [54,55] is displayed in Fig. 1A – the issues with other analyses are canvassed in Ref. [43]; and the K^-/π^- analysis from Ref. [15] is reproduced in Fig. 1B – these eight points represent all that is today known about the kaon structure function. We now use this information to produce data-driven estimates of pion and kaon DFs.

To begin, working with the E615 points drawn in Fig. 1A, we use least-squares minimisation to determine the parameters that produce a best fit in the form of Eq. (12), with the result:

$$[w_0^\pi] = \{\alpha_0, \beta_0, c_0^\pi\} = \{0.792, 2.71, 2.49\}\,. \tag{16}$$

It should be borne in mind that $\zeta = \zeta_5$ and $q = u = \bar{d}$. Furthermore, the large-x exponent, $\beta(\zeta_5) = 2.71 > 2$, is consistent with QCD-based expectations [43,47,52,56–58].

We now take the following steps.

(*I*) Generate a set of new vectors $\{[w_j^\pi]\,|\,j = 1,\ldots,N_w\}$, each element of which is distributed randomly around the best-fit result and accepted into a reference ensemble according to the probability

$$\mathcal{P} = \frac{P(\chi^2;d)}{P(\chi_0^2;d)}\,,\ P(y;d) = \frac{(1/2)^{d/2}}{\Gamma(d/2)}\, y^{d/2-1}\mathrm{e}^{-y/2}\,, \tag{17}$$

where

$$\chi^2([w_j^\pi]) = \frac{1}{\sigma}\sum_{i=1}^{M_{\rm E615}} \frac{[u^\pi(x_i;[w_j^\pi];\zeta_5) - u_i^{\rm E615}]^2}{\delta_i^2}\,; \tag{18}$$

$\{(x_i, u_i \pm \delta_i)\,|\,i = 1,\ldots,M_{\rm E615}\}$ are the points associated with the E615 data; and σ is a rescaling factor that ensures $\chi^2([w_0^\pi]) = d - 2$, making this the maximum of the probability density.

(*II*) Recalling that π, K valence quark DFs are characterised by the same values of α, β, define

$$R^{K/\pi}\left(x_j;[v_j^{K/\pi}];\zeta_5\right) = \frac{u^K(x_j;[w_K^j];\zeta_5)}{u^\pi(x_j;[w_\pi^j];\zeta_5)}\,, \tag{19}$$

which is the ratio depicted in Fig. 1B. Here, $[v_j^{K/\pi}] = \{\alpha_j, \beta_j, c_j^\pi, c_j^K\}$ is drawn from $[w_j^\pi] = \{\alpha_j, \beta_j, c_j^\pi\}$, $[w_j^K] = \{\alpha_j, \beta_j, c_j^K\}$. The single unfixed parameter is c_j^K in $u^K(x;\zeta_5)$. Using Eq. (13), it is determined by $\langle x\rangle_{u^K}^{\zeta_5}$.

(*III*) For a given pion configuration, $[w_j^\pi]$, consider an associated kaon DF defined by $[w_j^K]$ with c_j^K distributed randomly around a best fit value determined by the K/π points drawn in Fig. 1B and accepted into the reference ensemble with probability

$$\mathcal{P}_{R^{K/\pi}} = \mathcal{P}_{R^{K/\pi}|u^\pi}\,\mathcal{P}_{u^\pi}\,, \tag{20}$$

where $\mathcal{P}_{u^\pi}$ is the Step (*I*) acceptance probability and $\mathcal{P}_{R^{K/\pi}|u^\pi}$ is calculated using Eq. (17) with Eq. (18) amended so that $R^{K/\pi}\left(x_j;[v_j^{K/\pi}];\zeta_5\right)$ becomes the first term within the numerator parentheses and the reference values and uncertainties are the $M_{K/\pi} = 8$ points from Ref. [15]. Unsurprisingly, $\mathcal{P}_{R^{K/\pi}|u^\pi} \equiv \mathcal{P}_{u^K|u^\pi}$, so $\mathcal{P}_{u^K} = \mathcal{P}_{R^{K/\pi}}$; to wit, given u^π, then the acceptance probability of a K/π ratio is equivalent to that for u^K.

Beginning with $N_w = 200$ and following Steps (I - III), we arrive at a 111 member reference ensemble for $u^\pi(x;\zeta_5)$ and a 67 member ensemble for $u^K(x;\zeta_5)$. All members of both ensembles are displayed in Fig. 1A; and the associated ensemble of K/π ratios is drawn in Fig. 1B.

A key reference result is the replica averaged value of $\langle x\rangle_{u^\pi}^{\zeta_5} = 0.207(4)$. Within mutual uncertainties, this value matches the CSM prediction [22]: 0.20(2); and an average of mutually consistent lQCD results for this first moment [44,59–62]: 0.214(25). Of similar importance are the endpoint values of the ratio replicas drawn in Fig. 1B:

$$\begin{array}{lll} & x\to 0 & x\to 1 \\ \dfrac{u^K(x;\zeta_5)}{u^\pi(x;\zeta_5)} & 1.050(24) & 0.77(11) \end{array}\,. \tag{21}$$

These results match the predictions in Ref. [22], reproduced in Eq. (15). Plainly, more precise data are needed in order to reduce the $x \simeq 1$ uncertainty.

Using the AO scheme, each of the $u^M(x;\zeta_5)$ DF replicas can be evolved back to $\zeta_\mathcal{H}$ using the replica value of $\langle x\rangle_{u^\pi}^{\zeta_5}$. (We record the $\langle x\rangle_{u^\pi}^{\zeta_5}$ value associated with each accepted $R^{K/\pi}$.) To be clear, beginning with Eq. (11), one calculates the $\zeta_5 \to \zeta_\mathcal{H}$ Mellin moments for a given replica, j, then minimises the following functional over (ρ_M^j, γ_M^j):

$$\sum_{m=1}^{n_m}\left[\langle x^m\rangle_{u^M(\rho_M^j,\gamma_M^j)}^{\zeta_\mathcal{H}}/\mathcal{M}_M^j(m) - 1\right]^2\,, \tag{22}$$

where $\mathcal{M}_M^j(m)$ is the $\zeta_5 \to \zeta_\mathcal{H}$-evolved m$^{\rm th}$ Mellin moment of DF replica j. ($n_m = 10$ is sufficient for accurate reconstruction and $\gamma_\pi^j \equiv 0$ in Eqs. (4), (5).) The resulting ensembles of $\zeta_\mathcal{H}$ DFs are drawn in Fig. 2. Using Eq. (4), the parameter averages and dispersions are

$$\rho_\pi = 0.051(15)\,,\quad \rho_K = 0.054(13)\,, \gamma_K = 0.23(12)\,. \tag{23}$$

If one instead chooses Eq. (5), then, naturally, $\tilde{\rho}_\pi = \rho_\pi$, and $\tilde{\rho}_K = 0.044(13)$, $\tilde{\gamma}_K = 14(9)$.

A DF analogue of the asymptotic meson distribution amplitude, *viz.* $\varphi_{\rm as}(x) = 6x(1-x)$ [63–65], is the function $q_{\rm sf}(x) = 30x^2(1-x)^2$. Compared with this profile, EHM is expressed in the dilation of each replica in the DF ensembles drawn in Fig. 2. One notes from Fig. 2 that the CSM predictions for pion and kaon valence DFs [22] are consistent with the data-based inferences obtained herein, although the replica spreads, which owe to the imprecision of available data, diminish the significance of this correspondence.

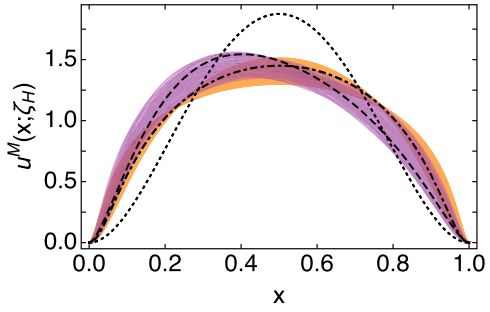

Fig. 2. Hadron-scale evolved ensembles of pion (orange) and kaon (purple) valence u quark DFs obtained following the procedure discussed in connection with Eq. (22). Dot-dashed (π) and dashed (K) curves are the predictions for these DFs in Ref. [22]. Dotted curve is the scale-free DF $q_{\rm sf}(x) = 30x^2(1-x)^2$.

Continuing with the discussion of Fig. 2, the peak location of each pion replica is $x = 1/2$. In contrast, the u^K replicas peak at $x = 0.42(4)$. This relative shift reflects the impact of Higgs boson couplings into QCD on the lighter quark sector [23]. Notably, $0.5/0.42(4) = 1.20(11)$ and the kaon-to-pion leptonic decay constant ratio is $f_K/f_\pi = 1.19$ [66]. The similarity between the values of these ratios highlights their common origin and the fact that even though the s quark current mass is 27-times greater than the average light-quark mass [66], this is largely masked in kaon observables by the scale of EHM.

Regarding $\langle x \rangle_{u^K}^{\zeta_{\mathcal{H}}}$, one may ($a$) calculate the hadron-scale valence u quark momentum fraction by using AO evolution $\zeta_5 \to \zeta_{\mathcal{H}}$ on the first moment of each of the 67 ζ_5 replicas indicated by Fig. 1. Equally, one may (b) follow the procedure discussed in connection with Eq. (22) to reconstruct $u^K(x;\zeta_{\mathcal{H}})$ and calculate the first moment of the result. These two approaches yield mutually consistent values:

$$\begin{array}{cc} (a) & (b) \\ \langle x \rangle_{u^K}^{\zeta_{\mathcal{H}}} \;\; 0.473(13) & 0.477(12) \end{array}, \tag{24}$$

which is a signal of the efficacy of our DF reconstruction procedure.

According to Ref. [58], the $x = 1$ value of the ratio $u^K(x;\zeta)/u^\pi(x;\zeta)$ is independent of ζ. At $\zeta_{\mathcal{H}}$, using Eq. (4):

$$R_1^{K/\pi}(\zeta_{\mathcal{H}}) = \lim_{x\to 1} \frac{u^K(x;\zeta_{\mathcal{H}})}{u^\pi(x;\zeta_{\mathcal{H}})} = \frac{n_0(\rho_K,\gamma_K)}{n_0(\rho_\pi,0)} \frac{\rho_\pi^2}{\rho_K^2}[1-\gamma_K]. \tag{25}$$

Inserting the DF reconstruction values from Eq. (23), one obtains $R_1^{K/\pi}(\zeta_{\mathcal{H}}) = 0.72(29)$, which matches the ζ_5 value in Eq. (21). As another test of $R_1^{K/\pi}$ scale invariance, we separately considered each calculated hadron-scale replica $u^{K,\pi}(x;\zeta_{\mathcal{H}})$, evolved it to $\zeta = \zeta_2 = 2$ GeV and $\zeta = \zeta_5$, then calculated and compared the $x \simeq 1$ ratio at these two scales. Over the 67 independent replicas that could be used, the mean difference $R_1^{K/\pi}(\zeta_2)$ *cf.* $R_1^{K/\pi}(\zeta_5)$ is just 1.6%. These levels of agreement, with discrepancies far smaller than statistical uncertainties, are strong evidence in support of scale invariance for the endpoint ratio in Eq. (25).

5. Complete set of kaon and pion DFs

Having now built hadron scale valence DFs for the pion and kaon, *viz.* $u^{\pi,K}(x;\zeta_{\mathcal{H}})$ and $\bar{s}^K(x;\zeta_{\mathcal{H}}) = u^K(1-x;\zeta_{\mathcal{H}})$, all glue and sea DFs in these mesons can also be obtained via AO evolution. In practice, we use the valence + singlet coupled system specified by Eqs. (5) in Ref. [37], with the hadron scale valence profiles as the initial surfaces, to produce n_m Mellin moments of each DF at the desired scale $\zeta > \zeta_{\mathcal{H}}$. As in Ref. [37], we employ quark-mass threshold functions to ensure that a given quark flavour only participates in evolution after the resolving scale exceeds $\epsilon_q = \zeta_H + \delta_q$, with $\delta_u = \delta_d = 0$ and (in GeV) $\delta_s = 0.1$, $\delta_c = 0.9$, $\delta_b = 3.9$. These threshold values are inferred from CSM predictions of dressed quark mass functions and their values at infrared momenta – see, *e.g.*, Ref. [6, Fig. 2.5]. With inputs based on a quark + interacting-diquark Faddeev equation picture [47], this approach to quark mass thresholds predicts a small but measurable $c + \bar{c}$ light-front momentum fraction ($\approx 1.3\%$) in the proton at $\zeta = \zeta_2$. The pointwise form of each DF is subsequently obtained by following a procedure analogous to that discussed in connection with Eq. (22), but using numerator Mellin moments associated with Eq. (12).

Employing this approach and working from the ensembles in Fig. 2, we obtain the $\zeta = \zeta_2, \zeta_5$ data-driven predictions for kaon valence DFs depicted in Fig. 3. They are described by Eq. (12) with the coefficients listed in Table 1. These valence DFs yield the light-front momentum fractions listed in Table 2, which express the fact that the $\bar{s}^K$ profile peaks at larger x than u^K owing to Higgs boson modulation of EHM. Moreover,

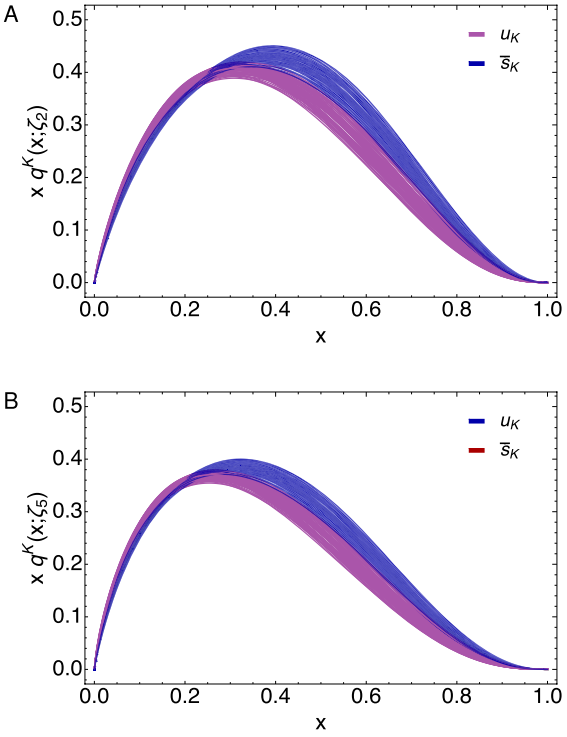

Fig. 3. Data-driven ensemble predictions for valence quark DFs in the kaon: Panel A – ζ_2; and Panel B – ζ_5.

Table 1
Used with Eq. (12), these coefficients deliver efficacious representations of all kaon DFs. The uncertainties express the statistical variation over input valence ensembles. For valence DFs, N_0 is fixed by baryon number conservation, but it is a free least-squares fitting parameter for sea and glue DFs.

	N_0	α	β	c^K
ζ_2				
u	2.48(23)	0.88(3)	2.42(12)	1.38(27)
$\bar{s}$	2.36(14)	0.90(3)	2.39(11)	2.56(43)
$u\bar{u}, d\bar{d}$	0.0298(7)	-0.544(5)	4.33(8)	0
$s\bar{s}$	0.0267(7)	-0.555(5)	4.36(8)	0
$c\bar{c}$	0.0065(1)	-0.618(4)	4.43(8)	0
g	0.384(11)	-0.566(5)	3.31(8)	0
ζ_5				
u	2.22(18)	0.79(3)	2.67(12)	1.20(24)
$\bar{s}$	2.26(15)	0.83(3)	2.65(11)	2.16(33)
$u\bar{u}, d\bar{d}$	0.0310(7)	-0.605(4)	4.67(9)	0
$s\bar{s}$	0.0287(5)	-0.613(4)	4.69(9)	0
$c\bar{c}$	0.0128(3)	-0.664(3)	4.76(8)	0
$b\bar{b}$	0.0015(1)	-0.698(3)	4.78(8)	0
g	0.313(7)	-0.642(4)	3.60(8)	0

Table 2
Light-front momentum fractions for valence-, sea and glue (columns 1, 2, 3, respectively), at resolving scales ζ_2 and ζ_5, obtained from replicas in Fig. 2 by AO evolution. For valence degrees-of-freedom, the first uncertainty is statistical and the second expresses a ±5% variation in $\zeta_{\mathcal{H}}$. In all other cases, the statistical error is negligible. For context, pion valence momentum fractions are given in the final column. Ignoring flavour dependence in nonsinglet evolution equations, pion sea and glue fractions are the same as those in the kaon – see Table 3.

	$\langle x\rangle^{\zeta}_{q^K}$	$\langle x\rangle^{\zeta}_{S^K_q}$	$\langle x\rangle^{\zeta}_{g^K}$	$\langle x\rangle^{\zeta}_{q^\pi}$
ζ_2				
u	0.230(6)(10)	0.028(2)		0.241(5)(10)
d	0	0.028(2)		0.241(5)(10)
s	0.252(6)(11)	0.026(1)		
c	0	0.008(1)		
b	0	0		
g			0.428(18)	
ζ_5				
u	0.197(5)(9)	0.036(2)		0.207(4)(9)
d	0	0.036(2)		0.207(4)(9)
s	0.216(5)(9)	0.034(2)		
c	0	0.019(1)		
b	0	0.003(1)		
g			0.461(20)	

Table 3
Data-driven light-front momentum fractions calculated at ζ_2 herein compared with available kindred results from lQCD [32]. l indicates the total fraction carried by light (u, d) quarks in the meson.

	empirical		[32, lQCD]	
M	π	K	π	K
l	0.538(15)	0.286(12)	0.499(55)	0.317(19)
s	0.026(01)	0.278(13)	0.036(15)	0.339(11)
c	0.008(01)	0.008(01)	0.013(16)	0.028(21)
q	0.572(15)	0.572(18)	0.575(79)	0.683(50)
g	0.428(18)	0.428(18)	0.402(53)	0.422(67)

like nucleons, a measurable component of pion and kaon light-front momentum is carried by the $c+\bar{c}$ sea.

The modest size of the relative shifts in the peak locations of pion, u-in-kaon and $\bar{s}$-in-kaon DFs is highlighted by Fig. 4 – see the three rightmost points, which depicts a collection of Mellin moment ratios and compares the values inferred herein, from results reported in Refs. [15,53], with CSM [22] and lQCD [61,67,68] predictions for these same ratios. A merit of such a comparison is that, *e.g.*, lQCD analyses can typically only deliver a few low-order moments, so objective conclusions can be drawn without reference to potentially subjective DF reconstruction using only a few moments. Evidently, the CSM predictions [22] are well aligned with the empirical results, whereas available lQCD values [61,67,68] tend to lie low when higher u quark moments are involved. This may indicate an underestimate of the larger-x support in the u quark DFs computed using lQCD. It should be noted that the lQCD results depicted in Fig. 4 were obtained with a pion mass $m_\pi = 0.26$ GeV at a lattice spacing $a = 0.093$ fm. No attempts were made in Refs. [61,67,68] to reach the physical pion mass or the continuum limit. Related improvements are underway [32].

The kaon sea and glue profiles are drawn in Fig. 5. Their pointwise forms are recovered by using Eq. (12) and the appropriate coefficients from Table 1. Notably, $\beta_{\rm sea} \approx \beta_{\rm glue} + 1 \approx \beta_{\rm valence} + 2$, in accordance with QCD-based expectations [56]. It is worth stressing that all DF ensembles drawn in Figs. 3, 5 are determined solely by empirical information on u^π, u^K and AO evolution. No model or theory of meson structure has been assumed/employed. The light-front momentum fraction carried by each species is listed in Table 2.

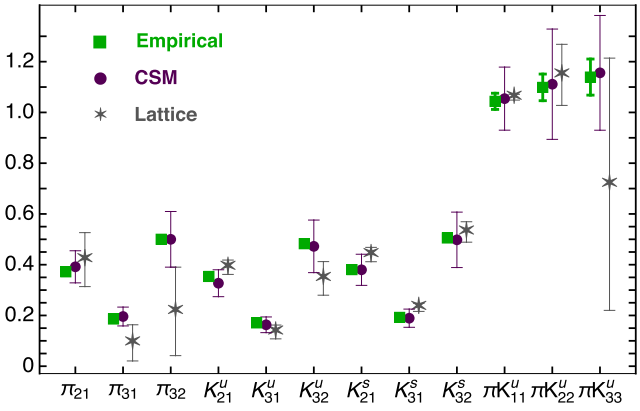

Fig. 4. Quark flavour-separated singlet Mellin moment ratios for the pion and kaon at ζ_2. Legend. $\pi_{ij} = \langle x^i\rangle_{u^\pi_S}/\langle x^j\rangle_{u^\pi_S}$, $K^q_{ij} = \langle x^i\rangle_{q^K_S}/\langle x^j\rangle_{q^K_S}$, $\pi K^u_{ij} = \langle x^i\rangle_{u^\pi_S}/\langle x^j\rangle_{u^K_S}$; "Empirical" – results inferred herein from Refs. [15,53], "CSM" – predictions from Ref. [22], "Lattice" – lQCD results from Ref. [61,67,68].

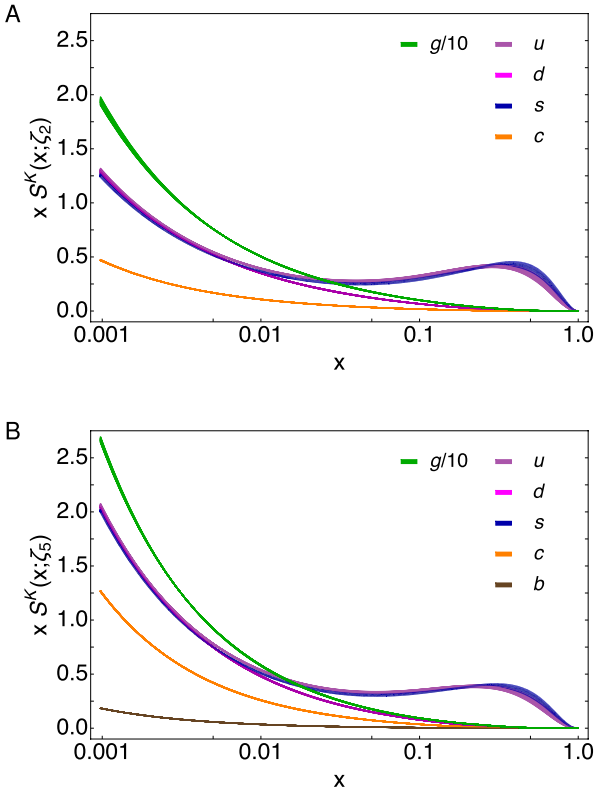

Fig. 5. Sea and glue DFs obtained via AO evolution of the kaon valence DF ensembles: Panel A – ζ_2; and Panel B – ζ_5. $b+\bar{b}$ sea contributions only appear in Panel B because ζ_2 lies below the b quark flavour threshold.

We have already highlighted that the data-driven predictions for pion and kaon DFs delivered herein are consistent with modern CSM predictions [22]. It is also interesting to compare them with available information from lQCD studies. In recent work, Ref. [32] used three gauge-field ensembles generated with 2 + 1 + 1-flavours of Wilson fermions at physical quark current masses and subsequently extrapolated to the continuum limit to provide an array of species separated light-front momentum fractions in the pion and kaon. They are reproduced in Table 3 and compared with like results from our analysis. Within mutual uncertainties, which are sizeable for the lQCD results (≈ 20% for pion and

$\approx 10\%$ for kaon, when the signal is strong), the level of agreement is fair and there are no striking discrepancies, especially when one accounts for the central-value violation of the momentum sum rule in the lQCD study. Nothing more can be said before uncertainties on the lQCD results are reduced.

It is worth reiterating that the light-front momentum fractions listed in Table 2 do not depend on details concerning the x-dependence of $u^{\pi,K}(x,\zeta_{\mathcal{H}})$. Instead, their values are completely determined by the fact that $\langle x\rangle^{\zeta_{\mathcal{H}}}_{u^\pi} + \langle x\rangle^{\zeta_{\mathcal{H}}}_{\bar{s}^\pi} \equiv 1$ and capitalisation on this feature via AO evolution. Consequently, the values in Table 2 – columns 2 and 3 are predictions of the AO method, as are the total quark and glue momentum fractions reported in Table 3. Under AO evolution, the momentum fractions carried by sea and glue are hadron independent [37,47], unless the nonsinglet splitting kernels are modified as discussed now.

In using AO evolution hitherto, we have neither implemented Pauli blocking [46,47] nor quark current-mass dependence in evolution of valence DFs [22, Sec. 7.3]. Consequently, the glue and flavour-summed quark momentum fractions listed in Tables 2, 3 are the same in the pion and kaon. Were we to follow Ref. [22, Sec. 7.3] in implementing mass dependence in valence DF evolution, then, *e.g.*, valence $\bar{s}$ quarks would produce less gluons than valence u quarks and gluon splitting would produce less $s+\bar{s}$ pairs than light-quark pairs. In consequence, we would obtain

$$\langle x\rangle^{\zeta}_{g^K} = \begin{cases} 0.4249(2)(180) & \zeta = 2\,\text{GeV} \\ 0.4582(2)(200) & \zeta = 5\,\text{GeV} \end{cases} . \tag{26}$$

(Uncertainties are statistical and $\zeta_{\mathcal{H}} \to (1\pm 0.05)\zeta_{\mathcal{H}}$ systematic.) Compared with the results in Table 2, the differences are within existing uncertainties. This explains why we have neglected the effect herein. Similar statements hold for Pauli blocking in the π and K – see the analysis in Ref. [37].

It is worth recording here that a suggestion [69] that the pion contains much more glue than the kaon was predicated on early fits to π-nucleon Drell-Yan data [70]. Relative to contemporary CSM predictions and the analysis described herein, those fits placed too little momentum with the pion's valence degrees of freedom, thereby misguiding the analysis in Ref. [69]. The modern picture indicates [22] that the in-kaon gluon momentum fraction is just 1% less than that in the pion – compare Eq. (26) with Table 3 – Row 5.

6. Summary and perspective

We described an approach to the reconstruction of pointwise profiles for all pion and kaon parton distribution functions (DFs) from valence parton DFs inferred via phenomenological analyses of relevant data. The key elements are data-constrained probability-weighted ensembles of valence DF replicas and the all-orders (AO) evolution scheme. The latter is crucial because it enables valence DFs to be brought together at a common hadron scale and thereat used as the initial value profiles in coupled evolution equations for all parton species.

Herein, one aim was to reveal what could be learnt from existing data (eight imprecise points) on the u-quark-in-kaon to u-quark-in-pion structure function ratio, $R^{K/\pi} = u^K(x)/u^\pi(x)$, when combined with available pion valence DF information derived from π-nucleon Drell-Yan measurements. Regarding the valence DFs and considering K^+ as the exemplar, the ensembles obtained express qualitatively sound features of kaon structure, such as the size of the relative shift in u and $\bar{s}$ DF peak locations caused by Higgs boson couplings into QCD [Fig. 3] and reasonably tight constraints on the associated light-front momentum fractions [Table 2]. Similar statements are applicable to all singlet DFs [Figs. 4, 5]. Of some interest are the results that the $c+\bar{c}$ sea carries approximately 2% of the kaon's light-front momentum at resolving scale $\zeta_5 = 5.2\,\text{GeV}$, with $\approx 0.3\%$ carried by $b+\bar{b}$ [Table 2].

An open question is what data should be collected in order to aid in delivering more refined statements about kaon and pion structure. Most simply, more, precise data on $R^{K/\pi}$ would be valuable. At present, the u^K and $\bar{s}^K$ valence DF ensembles obtained therefrom overlap on large x domains; so, the true size of EHM modulation by Higgs boson couplings into QCD is unclear. More valuable still would be extraction of u^K alone, *i.e.*, avoiding inference from $R^{K/\pi}$. At present, the extracted form of u^K is too much influenced by results for, or assumptions about, u^π. Many calculations have shown that the same $R^{K/\pi}$ profile is produced by distinctly different, yet internally consistent, results for $u^{K,\pi}$ – see, *e.g.*, Ref. [22, Fig. 12], which contrasts a CSM prediction of the ratio with a lQCD result [24]. Such data is anticipated in the foreseeable future [6,16–20].

Declaration of competing interest

The authors declare that they have no known competing financial interests or personal relationships that could have appeared to influence the work reported in this paper.

Acknowledgements

Work supported by: National Natural Science Foundation of China (grant no. 12135007, 12247103); Spanish Ministry of Science, Innovation and Universities (MICIU grant no. PID2022-140440NB-C22); Program d'Alembert of the Université de Paris-Saclay; Project AST22_00001_X, funded by NextGenerationEU and "Plan de Recuperación, Transformación y Resiliencia y Resiliencia" (PRTR) from MICIU and Junta de Andalucía; and completed in part at Institut Pascal, Université Paris-Saclay, with the support of the program "Investissements d'avenir" ANR-11-IDEX-0003-01.

Data availability

Data will be made available on request.

References

[1] G.D. Rochester, C.C. Butler, Evidence for the existence of new unstable elementary particles, Nature 160 (1947) 855–857.
[2] R. Brown, U. Camerini, P.H. Fowler, H. Muirhead, C.F. Powell, D.M. Ritson, Observations with electron sensitive plates exposed to cosmic radiation, Nature 163 (1949) 82.
[3] M. Gell-Mann, A. Pais, Behavior of neutral particles under charge conjugation, Phys. Rev. 97 (1955) 1387–1389.
[4] M. Bardon, K. Lande, L.M. Lederman, W. Chinowsky, Long-lived neutral K mesons, Ann. Phys. 5 (2) (1958) 156–181.
[5] C.M.G. Lattes, H. Muirhead, G.P.S. Occhialini, C.F. Powell, Processes involving charged mesons, Nature 159 (1947) 694–697.
[6] C.D. Roberts, D.G. Richards, T. Horn, L. Chang, Insights into the emergence of mass from studies of pion and kaon structure, Prog. Part. Nucl. Phys. 120 (2021) 103883.
[7] D. Binosi, Emergent hadron mass in strong dynamics, Few-Body Syst. 63 (2) (2022) 42.
[8] M. Ding, C.D. Roberts, S.M. Schmidt, Emergence of hadron mass and structure, Particles 6 (1) (2023) 57–120.
[9] M.N. Ferreira, J. Papavassiliou, Gauge sector dynamics in QCD, Particles 6 (1) (2023) 312–363.
[10] D.S. Carman, R.W. Gothe, V.I. Mokeev, C.D. Roberts, Nucleon resonance electroexcitation amplitudes and emergent hadron mass, Particles 6 (1) (2023) 416–439.
[11] K. Raya, A. Bashir, D. Binosi, C.D. Roberts, J. Rodríguez-Quintero, Pseudoscalar mesons and emergent mass, Few-Body Syst. 65 (2) (2024) 60.
[12] T. Horn, C.D. Roberts, The pion: an enigma within the standard model, J. Phys. G 43 (2016) 073001.
[13] Z.-F. Cui, D. Binosi, C.D. Roberts, S.M. Schmidt, Pion charge radius from pion+electron elastic scattering data, Phys. Lett. B 822 (2021) 136631.
[14] M. Carmignotto, et al., Separated kaon electroproduction cross section and the kaon form factor from 6 GeV JLab data, Phys. Rev. C 97 (2018) 025204.
[15] J. Badier, et al., Measurement of the K^-/π^- structure function ratio using the Drell-Yan process, Phys. Lett. B 93 (1980) 354.
[16] K. Park, R. Montgomery, T. Horn, et al., Measurement of Kaon Structure Function through Tagged Deep Inelastic Scattering (TDIS) approved Jefferson Lab experiment C12-15-006A.
[17] X. Chen, F.-K. Guo, C.D. Roberts, R. Wang, Selected science opportunities for the EicC, Few-Body Syst. 61 (2020) 43.
[18] J. Arrington, et al., Revealing the structure of light pseudoscalar mesons at the electron–ion collider, J. Phys. G 48 (2021) 075106.

[19] B. Seitz, AMBER: a new QCD facility at the CERN SPS M2 beam line, PoS ICHEP2022 (2023) 839.
[20] F. Metzger, et al., Kaon beam simulations employing conventional hadron beam concepts and the RF separation technique at the CERN M2 beamline for the future AMBER experiment, JACoW IPAC2023 (2023) TUPM070.
[21] A. Kock, Y. Liu, I. Zahed, Pion and kaon parton distributions in the QCD instanton vacuum, Phys. Rev. D 102 (1) (2020) 014039.
[22] Z.-F. Cui, M. Ding, F. Gao, K. Raya, D. Binosi, L. Chang, C.D. Roberts, J. Rodríguez-Quintero, S.M. Schmidt, Kaon and pion parton distributions, Eur. Phys. J. C 80 (2020) 1064.
[23] Z.-F. Cui, M. Ding, F. Gao, K. Raya, D. Binosi, L. Chang, C.D. Roberts, J. Rodríguez-Quintero, S.M. Schmidt, Higgs modulation of emergent mass as revealed in kaon and pion parton distributions, Eur. Phys. J. A 57 (1) (2021) 5.
[24] H.-W. Lin, J.-W. Chen, Z. Fan, J.-H. Zhang, R. Zhang, Valence-quark distribution of the kaon and pion from lattice QCD, Phys. Rev. D 103 (1) (2021) 014516.
[25] G. Xie, C. Han, R. Wang, X. Chen, Tackling the kaon structure function at EicC, Chin. Phys. C 46 (6) (2022) 064107.
[26] J.M.M. Chávez, V. Bertone, F. De Soto Borrero, M. Defurne, C. Mezrag, H. Moutarde, J. Rodríguez-Quintero, J. Segovia, Accessing the pion 3D structure at US and China electron-ion colliders, Phys. Rev. Lett. 128 (20) (2022) 202501.
[27] W. de Paula, E. Ydrefors, J.H. Nogueira Alvarenga, T. Frederico, G. Salmè, Parton distribution function in a pion with Minkowskian dynamics, Phys. Rev. D 105 (7) (2022) L071505.
[28] B. Pasquini, S. Rodini, S. Venturini, Valence quark, sea, and gluon content of the pion from the parton distribution functions and the electromagnetic form factor, Phys. Rev. D 107 (11) (2023) 114023.
[29] X. Wang, M. Ding, L. Chang, Sieving parton distribution function moments via the moment problem, Phys. Lett. B 851 (2024) 138568.
[30] W. Good, K. Hasan, A. Chevis, H.-W. Lin, Gluon moment and parton distribution function of the pion from Nf = 2+1+1 lattice QCD, Phys. Rev. D 109 (11) (2024) 114509.
[31] W.-C. Chang, J.-C. Peng, S. Platchkov, T. Sawada, Constraining kaon PDFs from Drell-Yan and J/ψ production, Phys. Lett. B 855 (2024) 138820.
[32] C. Alexandrou, et al., Quark and gluon momentum fractions in the pion and in the kaon, arXiv:2405.08529 [hep-lat]. Herein, we employ results from an updated version of Table 2 in this reference, supplied in a private communication from C. Alexandrou.
[33] Y.L. Dokshitzer, Calculation of the structure functions for deep inelastic scattering and $e^+ e^-$ annihilation by perturbation theory in quantum chromodynamics, Sov. Phys. JETP 46 (1977) 641–653 (in Russian).
[34] V.N. Gribov, L.N. Lipatov, Deep inelastic electron scattering in perturbation theory, Phys. Lett. B 37 (1971) 78–80.
[35] L.N. Lipatov, The parton model and perturbation theory, Sov. J. Nucl. Phys. 20 (1975) 94–102.
[36] G. Altarelli, G. Parisi, Asymptotic freedom in parton language, Nucl. Phys. B 126 (1977) 298–318.
[37] P.-L. Yin, Y.-Z. Xu, Z.-F. Cui, C.D. Roberts, J. Rodríguez-Quintero, All-orders evolution of parton distributions: principle, practice, and predictions, Chin. Phys. Lett. 40 (9) (2023) 091201.
[38] G. Grunberg, Renormalization group improved perturbative QCD, Phys. Lett. B 95 (1980) 70; Phys. Lett. B 110 (1982) 501 (Erratum).
[39] G. Grunberg, Renormalization scheme independent QCD and QED: the method of effective charges, Phys. Rev. D 29 (1984) 2315.
[40] A. Deur, S.J. Brodsky, C.D. Roberts, QCD running couplings and effective charges, Prog. Part. Nucl. Phys. 134 (2024) 104081.
[41] Z.-F. Cui, J.-L. Zhang, D. Binosi, F. de Soto, C. Mezrag, J. Papavassiliou, C.D. Roberts, J. Rodríguez-Quintero, J. Segovia, S. Zafeiropoulos, Effective charge from lattice QCD, Chin. Phys. C 44 (2020) 083102.
[42] S.J. Brodsky, A. Deur, C.D. Roberts, The secret to the strongest force in the universe, Sci. Am. 5 (May 2024) 32–39.
[43] Z.F. Cui, M. Ding, J.M. Morgado, K. Raya, D. Binosi, L. Chang, J. Papavassiliou, C.D. Roberts, J. Rodríguez-Quintero, S.M. Schmidt, Concerning pion parton distributions, Eur. Phys. J. A 58 (1) (2022) 10.
[44] Y. Lu, Y.-Z. Xu, K. Raya, C.D. Roberts, J. Rodríguez-Quintero, Pion distribution functions from low-order Mellin moments, Phys. Lett. B 850 (2024) 138534.
[45] H.Y. Xing, Z.Q. Yao, B.L. Li, D. Binosi, Z.F. Cui, C.D. Roberts, Developing predictions for pion fragmentation functions, Eur. Phys. J. C 84 (1) (2024) 82.
[46] L. Chang, F. Gao, C.D. Roberts, Parton distributions of light quarks and antiquarks in the proton, Phys. Lett. B 829 (2022) 137078.
[47] Y. Lu, L. Chang, K. Raya, C.D. Roberts, J. Rodríguez-Quintero, Proton and pion distribution functions in counterpoint, Phys. Lett. B 830 (2022) 137130.
[48] P. Cheng, Y. Yu, H.-Y. Xing, C. Chen, Z.-F. Cui, C.D. Roberts, Perspective on polarised parton distribution functions and proton spin, Phys. Lett. B 844 (2023) 138074.
[49] Y. Yu, P. Cheng, H.-Y. Xing, F. Gao, C.D. Roberts, Contact interaction study of proton parton distributions, Eur. Phys. J. C 84 (7) (2024) 739.
[50] Z.Q. Yao, Y.Z. Xu, D. Binosi, Z.F. Cui, M. Ding, K. Raya, C.D. Roberts, J. Rodríguez-Quintero, S.M. Schmidt, Nucleon gravitational form factors, arXiv:2409.15547 [hep-ph].
[51] Y. Yu, C.D. Roberts, Impressions of parton distribution functions, Chin. Phys. Lett. 41 (2024) 121202.
[52] Z.F. Cui, M. Ding, J.M. Morgado, K. Raya, D. Binosi, L. Chang, F. De Soto, C.D. Roberts, J. Rodríguez-Quintero, S.M. Schmidt, Emergence of pion parton distributions, Phys. Rev. D 105 (9) (2022) L091502.
[53] J.S. Conway, et al., Experimental study of muon pairs produced by 252-GeV pions on tungsten, Phys. Rev. D 39 (1989) 92–122.
[54] M. Aicher, A. Schäfer, W. Vogelsang, Soft-gluon resummation and the valence parton distribution function of the pion, Phys. Rev. Lett. 105 (2010) 252003.
[55] L. Chang, C. Mezrag, H. Moutarde, C.D. Roberts, J. Rodríguez-Quintero, P.C. Tandy, Basic features of the pion valence-quark distribution function, Phys. Lett. B 737 (2014) 23–29.
[56] S.J. Brodsky, M. Burkardt, I. Schmidt, Perturbative QCD constraints on the shape of polarized quark and gluon distributions, Nucl. Phys. B 441 (1995) 197–214.
[57] F. Yuan, Generalized parton distributions at $x \to 1$, Phys. Rev. D 69 (2004) 051501.
[58] R.J. Holt, C.D. Roberts, Distribution functions of the nucleon and pion in the valence region, Rev. Mod. Phys. 82 (2010) 2991–3044.
[59] B. Joó, J. Karpie, K. Orginos, A.V. Radyushkin, D.G. Richards, R.S. Sufian, S. Zafeiropoulos, Pion valence structure from Ioffe-time parton pseudodistribution functions, Phys. Rev. D 100 (2019) 114512.
[60] R.S. Sufian, J. Karpie, C. Egerer, K. Orginos, J.-W. Qiu, D.G. Richards, Pion valence quark distribution from matrix element calculated in lattice QCD, Phys. Rev. D 99 (2019) 074507.
[61] C. Alexandrou, S. Bacchio, I. Cloet, M. Constantinou, K. Hadjiyiannakou, G. Koutsou, C. Lauer, Pion and kaon $\langle x^3 \rangle$ from lattice QCD and PDF reconstruction from Mellin moments, Phys. Rev. D 104 (5) (2021) 054504.
[62] X. Gao, A.D. Hanlon, N. Karthik, S. Mukherjee, P. Petreczky, P. Scior, S. Shi, S. Syritsyn, Y. Zhao, K. Zhou, Continuum-extrapolated NNLO valence PDF of the pion at the physical point, Phys. Rev. D 106 (11) (2022) 114510.
[63] G.P. Lepage, S.J. Brodsky, Exclusive processes in quantum chromodynamics: evolution equations for hadronic wave functions and the form-factors of mesons, Phys. Lett. B 87 (1979) 359–365.
[64] A.V. Efremov, A.V. Radyushkin, Factorization and asymptotical behavior of pion form- factor in QCD, Phys. Lett. B 94 (1980) 245–250.
[65] G.P. Lepage, S.J. Brodsky, Exclusive processes in perturbative quantum chromodynamics, Phys. Rev. D 22 (1980) 2157–2198.
[66] S. Navas, et al., Review of particle physics, Phys. Rev. D 110 (3) (2024) 030001.
[67] C. Alexandrou, S. Bacchio, I. Cloet, M. Constantinou, K. Hadjiyiannakou, G. Koutsou, C. Lauer, Mellin moments $\langle x \rangle$ and $\langle x^2 \rangle$ for the pion and kaon from lattice QCD, Phys. Rev. D 103 (1) (2021) 014508.
[68] C. Alexandrou, Presentation at the CFNS Workshop: Elucidating the Structure of Nambu-Goldstone Bosons, Mon. 2024/06/24.
[69] C. Chen, L. Chang, C.D. Roberts, S. Wan, H.-S. Zong, Valence-quark distribution functions in the kaon and pion, Phys. Rev. D 93 (2016) 074021.
[70] M. Glück, E. Reya, I. Schienbein, Pionic parton distributions revisited, Eur. Phys. J. C 10 (1999) 313–317.